Geotechnical Testing Journal

doi:10.1520/GTJ20140215 / Vol. 38 / No. 5 / September 2015 / available online at www.astm.org

Jonathan A. Black[1] and Alireza Tatari[2]

Transparent Soil to Model Thermal Processes: An Energy Pile Example

Reference

Black, Jonathan A. and Tatari, Alireza, "Transparent Soil to Model Thermal Processes: An Energy Pile Example," *Geotechnical Testing Journal*, Vol. 38, No. 5, 2015, pp. 752–764, doi:10.1520/GTJ20140215. ISSN 0149-6115

ABSTRACT

Managing energy resources is fast becoming a crucial issue of the 21st century, with ground-based heat exchange energy structures targeted as a viable means of reducing carbon emissions associated with regulating building temperatures. Limited information exists about the thermo-dynamic interactions of geothermal structures and soil owing to the practical constraints of placing measurement sensors in proximity to foundations; hence, questions remain about their long-term performance and interaction mechanics. An alternative experimental method using transparent soil and digital image analysis was proposed to visualize heat flow in soil. Advocating the loss of optical clarity as a beneficial attribute of transparent soil, this paper explored the hypothesis that temperature change will alter its refractive index and therefore progressively reduce its transparency, becoming more opaque. The development of the experimental methodology was discussed and a relationship between pixel intensity and soil temperature was defined and verified. This relationship was applied to an energy pile example to demonstrate heat flow in soil. The heating zone of influence was observed to extend to a radial distance of 1.5 pile diameters and was differentiated by a visual thermal gradient propagating from the pile. The successful implementation of this technique provided a new paradigm for transparent soil to potentially contribute to the understanding of thermo-dynamic processes in soil.

Keywords

transparent soil, thermal modeling, energy pile, energy, image analysis

Manuscript received September 16, 2014; accepted for publication March 24, 2015; published online April 21, 2015.

[1] Senior Lecturer, Department of Civil and Structural Engineering, Univ. of Sheffield, Sheffield, S1 3JD, UK, e-mail: j.a.black@sheffield.ac.uk

[2] Ph.D. Research Student, Department of Civil and Structural Engineering, Univ. of Sheffield, Sheffield, S1 3JD, UK.

Nomenclature

CCD = charged couple device
cP = centipoises
d_0 = pile diameter
D = depth
dc = direct current
H = height
k = thermal conductivity
LED = light emitting diode
l = litres
lp/mm = line pair per mm
MTF = modulation transfer function
n = index of refraction
N = centrifuge acceleration scale
PI = pixel intensity
PID = proportional-integral-derivative
PI_N = normalized pixel intensity
PI_{max} = maximum pixel intensity
PI_{min} = minimum pixel intensity
PIV = particle image velocimetry
r = radius
RI = refractive index
SLR = single lens reflex
USB = universal serial bus
W = width
z = soil depth
°C = degree Celsius

Introduction

ENERGY GEOTECHNICS

Managing natural resources is becoming one of the crucial issues of the 21st century and is closely linked to the need to reduce our carbon footprint and become more energy sustainable. Geotechnical energy structures/foundations are believed to offer potential to make a positive contribution to this vision by serving as energy exchange systems to regulate building environmental conditions. In winter, the ground temperature is higher than the air and it therefore provides a potential source of heat energy; alternatively, in summer, the ambient air temperature is higher and the ground can be used as a heat sink to cool the building; thus reducing the reliance on conventional heating and cooling systems.

The concept of ground energy exchange systems has been proposed and implemented for decades, with Brandl (2006) reporting on the first installation of thermal piles in the 1980s. Despite this period since their initial deployment, design methods for their thermal or geotechnical aspects are not yet well established (Loveridge and Powrie 2012). The lack of a unified approach is largely attributed to the difficulties in optimizing heat exchange within an energy foundation, current understanding of the effects of temperature on soil behavior, and uncertainty of thermo-mechanical interactions. In this respect, although it is well known that soil behavior is influenced by temperature, the extent of the response is highly variable and dependent on particle size, mineralogy, and stress history of the soil. Many researchers conducted element tests to study the behavior of soils subjected to temperature changes. Campanella and Mitchell (1968) show that an increase in temperature in drained conditions produced a volume reduction of clay soil. Demars and Charles (1982) documented similar findings and reported that soil behavior was strongly dependent on the overconsolidation ratio in their investigation of a marine undisturbed clay. Similarly, Towhata et al. (1993) reported that normally consolidated clays exhibited thermal contractive behavior, whereas overconsolidated clays can show thermal dilatant behavior. Other studies related to the compression of normally consolidated clays include Mitchell 1964, Plum and Esrig (1969), Habibagahi (1977), and Boudali et al. (1994) who reported that the compression curves obtained at different temperatures are parallel, with lower values of void ratio at higher temperatures.

Variations in shear strength with temperature are also reported. For example, Hueckel et al. (2011) summarized that experimental studies of the triaxial strength of clays show that remolded kaolin clay and natural Boom Clay exhibit temperature dependence of their internal friction, whereas this is not the case for largely smectitic or illitic clays based on works by Hueckel and Baldi (1990) Hueckel and Pellegrini (1992), and Cekerevac and Laloui (2004). Conversely, Houston et al. (1985) reported increases in peak shear strength at elevated temperature under undrained conditions for an illitic and smectitic rich ocean sediment. Hueckel et al. (2009) demonstrated that although numerically small, a 10 % temperature-induced increase in the critical state coefficient M over 90°C can produce an increase in compressive strength of up to 25 %, compared with the case of a temperature-independent friction angle. Furthermore, it is noteworthy that Hueckel et al. (2011) reported the effects of the thermal variation of internal friction depend heavily on the history of heating and loading. This aspect could have considerable implications on the thermo-mechanical response of foundations (i.e., energy piles) deployed as energy structures, such that under working stress, deterioration of stability and serviceability could manifest, leading to uncertainty in long-term performance. In this respect, Loveridge and Powrie (2012) stated that while observations from trial energy pile tests at Lambeth College in London (reported by Bourne-Webb et al. 2009) suggest the thermo-mechanical response of the pile is reversible, these short term tests would not have identified smaller thermal loading cyclic effects that that could become significant over longer time scales and more heating/cooling cycles.

Owing to the complexity that surrounds assessing the likely thermo-mechanical performance of energy foundations, several

field investigations were conducted in an effort to enhance understanding of thermal response of energy structures in the ground. Laloui et al. (2003) conducted heating tests on a 1-m diameter energy pile embedded in saturated alluvial sandy soil under different working loads. Without any applied axial load, heating the pile by 21°C induced a heave of 3.5 mm and over 4 MPa of axial stress. Under working load conditions, a three-fold increase was recorded in the maximum axial load when the pile was subjected to a 14°C temperature increase. The most widely reported field tests are those previously introduced at Lambeth College, London by Bourne-Webb et al. (2009). The pile had a diameter of 0.55 m, length of 23 m, and was embedded in London clay. The pile was subjected to separate heating and cooling cycles while carrying a working load of 1200 kN. Heating caused an increase in pile axial load of up to 800 kN, while the cooling cycle led to a reduction in load of about 500 kN. Accompanying changes in pile head displacement were small at less than 2 mm. Other field investigations are reported by Wood et al. (2010), who investigated the heat pump performance on a test plot of 21 concrete test piles, 10 m deep for residential buildings. In addition, Pahud and Hubbuch (2007) measured thermal performances of an energy pile system deployed at Zurich Airport confirming that the observed performance was as intended. Gao et al. (2008) and Hepbasli et al. (2003) reported on studies that predominately focused on improving the efficiency and design of heat exchangers in the field. Finally, wider commentary on the broader use of geostructures as heat exchangers in the field such as diaphragm walls, thermal piles, and tunnels are reported by Brandl (2006).

While the above field studies were highly beneficial in providing some initial performance data of thermally active foundations, uncertainties in the assessment of energy foundations are exacerbated by the lack of high quality monitoring data from case studies on which to validate new approaches (Loveridge and Powrie 2012). Specifically, extensive long-term data relating to the thermo-dynamic interactions of geothermal heat exchange structures and soil is lacking owing to the practical constraints of placing measurement sensors in the soil in close proximity to the geostructure and the data collection time required. As demonstrated in the laboratory element tests, changes in soil characteristics with temperature could affect the performance of geostructures deployed as energy exchange systems. Potential issues could range from increased foundation movement due to the thermal expansion and contraction of the foundation or surrounding soil, or the build-up of internal thermal induced stresses, especially over multiple thermal cycles.

Although current field data is limited in duration and number of cycles achieved, several physical model studies were conducted in the centrifuge that evaluated longer-term impacts of multiple thermal cycles. This is possible owing to scaling laws derived by Savvidou (1988), who determined the time scaling factor of N^2 (N being the applied enhanced gravity in the centrifuge) for heat flow in accelerated gravity experiments, which enables multi thermal cycles to be simulated in a shorter duration (hours) that would normally take years at full field scale. Notable centrifuge investigations benefiting from this scaling relationship include Stewart and McCartney (2014), Ng et al. (2014), Britto et al. (1989), Goode et al. (2014), and Stewart and McCartney (2012). These studies considered a range of various soil types with reported observations of increased pile settlements and ratcheting over several thermal cycles. While this behavior has not been observed at full scale, its detection in simulated prototype field stress conditions within the centrifuge is disconcerting and echoes concerns by other authors that thermal loading cyclic effects could become significant over longer time scales and more heating/cooling cycles (Loverage and Powrie 2012). Hence, the long-term performance of energy foundations is not well understood and is likely to be the focus of considerable ongoing research in future studies in this field.

TRANSPARENT SOIL MODELING

Transparent soil consists of an aggregate and a matched refractive index fluid. When fully saturated, the particles appear invisible and allow light to pass, enabling visualization through the soil. Both fine (clay) and coarse-grained (sands/gravels) were developed and the materials and their mechanical properties are summarized by Iskander (2010). Many experiments in transparent soil focused on identifying aspects of fluid flow or mechanical response of the soil to enhance understanding of soil–structure interaction behavior (Iskander et al. 1994; Iskander et al. 2002; Sadek et al. 2002; Lui et al. 2002; Lui et al. 2002; Ezzein and Bathurst 2014). Investigations of this nature have sought to optimize soil transparency in order to accommodate models of increased geometry and offer greater visualization of tracking particles within the soil for displacement measurement. Gill (1999) used back illumination to silhouette embedded target markers; however, that has been superseded by modern laser aided imaging in conjunction with digital image correlation techniques (for example Sadek et al. 2003 and Hird et al. 2008). Works using this approach include examination of failure mechanics of helical screw piles (Stanier et al. 2013), stone column groups (Kelly 2013), and tunnel induced settlements (Ahmed and Iskander 2010) soil plugging behavior during press-in piling of tubular piles (Black 2012; Forlati and Black 2014).

The success of transparent soil modeling has long been considered reliant on producing a soil surrogate that offers the highest optical clarity, with low transparency being considered detrimental to the modeling technique (Black and Take 2015). However, recent work by Siemens et al. (2010) and Peters et al. (2011) embraced the loss of soil transparency as a positive characteristic for the purpose of modeling unsaturated soil phenomena. The authors appreciated that fused quartz soil particles

appeared white in color when dry, yet were invisible when submerged in suitably matched refractive index pore fluid (i.e., 100 % saturation), so that a uniform black background behind the soil would be clearly visible. Intermediate levels of saturation enable only partial transmission of light such that the calibration target no longer would appear uniform black, but gray/white in color at the fluid–air boundaries. Evaluating pixel intensity of the background from fully saturated to dry conditions enabled the authors to successfully correlate the degree of saturation from digital images. In doing so, the authors provided a new opportunity for transparent soil to offer complementary insight of unsaturated soil problems.

This paper also advocates the loss of optical clarity as a beneficial attribute of transparent soil, focusing on the property of refractive index and its temperature dependency for the purpose of viewing heat flow in soil to model thermo-dynamic problems. It is hypothesized that temperature changes will have a negative impact on soil transparency and the soil will become progressively more opaque as the temperature deviates from the optimum calibrated refractive index match. Hence, changes in transparency can be registered as a shift in pixel intensity of a black background viewed through the soil, which can be related to temperature variations. The aim of this paper is to provide a comprehensive overview of the novel testing protocol that has been developed to fulfil this hypothesis, and to define a relationship for pixel intensity and temperature. The potential for transparent soil to model thermo-dynamic processes is demonstrated using an energy pile application whereby heat flow is quantified through direct visualization and coupled with image analysis.

Concept of Visualising Heat in Transparent Soil

REFRACTIVE INDEX

Refractive index, also called index of refraction (n), is a dimensionless number that describes how light propagates through a medium and is defined as a ratio of the speed of light in the medium relative to its speed in a vacuum. It is also important to note that light changes direction when it travels from one medium to another whereby Snell's law can be used to determine the angle of incidence and refraction. Refractive index of a material is affected by factors such as the wavelength of light and temperature. For this reason, refractive index properties of materials are quoted with respect to the temperature at which they were determined. Variation in temperature affects material density, which in turn affects the speed of light; therefore, increased refraction and dispersion of light rays occur, which manifest as a loss of transparency such that a previously transparent medium may appear as less clear or become opaque as temperature changes.

IMAGE ANALYSIS METHODOLOGY

Individual pixels are the smallest addressable element that combines to form a digital image as a two-dimensional representation of a real object. Each pixel within the image has a pixel intensity value that describes its brightness and color. The most common pixel format is where the pixel number is stored as an 8-bit integer with a range of possible values from 0 (black) to 255 (white). Values in between these extremes describe the spectrum of shades of gray. In color images, separate red, green, and blue components must be specified for each pixel; hence the pixel value is actually a vector of the three individual pixel intensity numbers.

Referring to **Fig. 1**, when a uniform black background is placed behind transparent soil mixed at its optimum refractive match for a given temperature (i.e., calibrated at 20°C), it will be visible as the soil is transparent and allows the passage of light; therefore, pixel intensities representative of black would be returned in an image. Examining the pixel intensity of a subregion would reveal that the pixel intensity values are not truly black (i.e., zero), but are still sufficiently low to be portrayed as black in the image. It is not uncommon in digital images that the true color information from a real object will not be perfectly transferred to an image due to aberrations and diffraction

FIG. 1

Concept of pixel–temperature visual based measurement for thermal modeling applications in transparent soil.

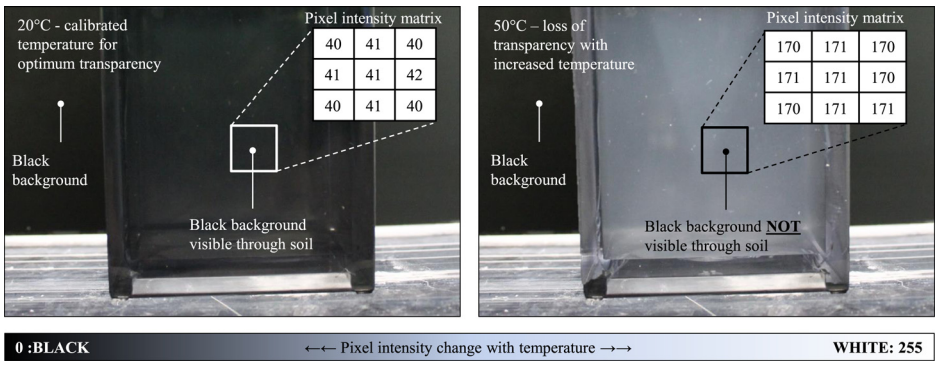

FIG. 2

Concept of using signal modulation to detect changes in contrast from changing refractive index due to temperature changes (*a*) demonstration using artificial image and (*b*) verification in transparent soil.

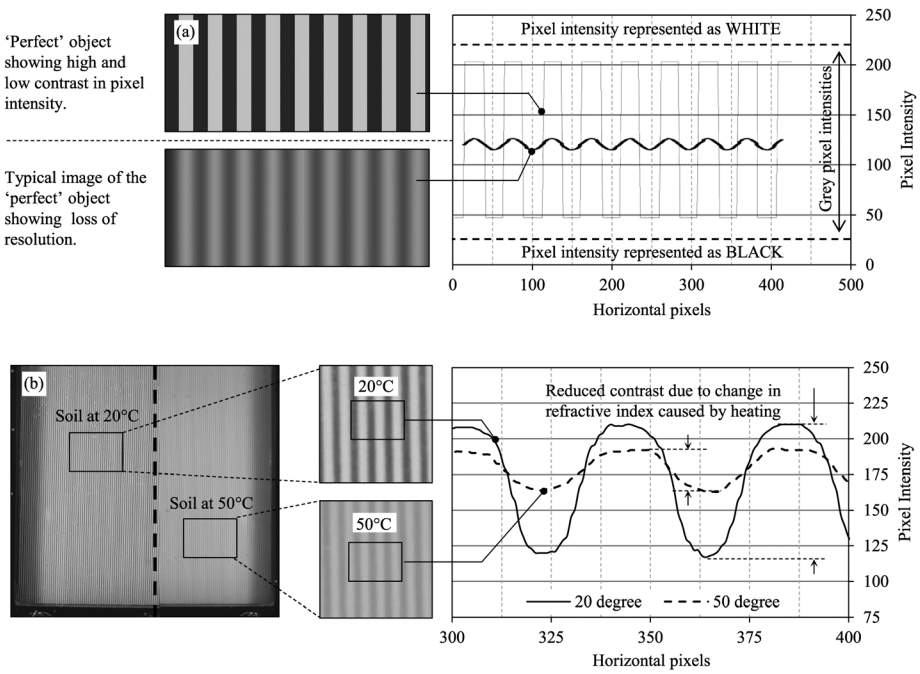

caused by the camera and lens, illumination conditions, or in this instance, viewing the target through a translucent medium. Conversely, if the soil temperature was increased (i.e., to 50°C) the refractive index would change and reduce light transmission; therefore, the black target will be less visible or fully obscured. In this instance, the pixel intensity would no longer be close to zero, but increase such that the soil would be considered to be gray in color. Observed changes in pixel intensity provide a clear basis on which to establish a direct visual assessment measurement to detect temperature changes in transparent soil captured in digital images.

The background (referred to herein as "calibration target") implemented in the current research consisted of two distinct regions: (i) black uniform intensity and (ii) alternating black and white stripes at a spatial frequency of 1 line pair per mm (lp/mm). This split target was adopted due to the positive outcome in the work of Siemens et al. (2010) and Peters et al. (2011), who reported success using a black uniform background to detect changes in pixel intensity to capture loss of optical transmission, and striped region due to complementary work by Black and Take (2015) that established a robust quantitative framework for assessing the optical quality of transparent soils using optical method referred to as "modulation transfer function" (MTF). MTF operates by relating the pixel contrast that is transferred from an object to an image and is commonly used to calibrate optical systems. When the transparent soil is of high quality and well optically matched, the modulation contrast between the minimum (black) and maximum (white) pixel intensity is well-defined. However, if transparency is poor or diminishes, then contrast reduces towards a single pixel intensity value (i.e., image blends to gray color). The loss in signal modulation is governed by the transparency; hence, MTF can be used to quantify and evaluate the reduction in clarity that occurs as temperature changes. This process is fully described in Black and Take (2015); however, the main principle is conveyed in **Fig. 2**, which demonstrates the loss in modulation when temperature increases in transparent soil. This approach offers an alternative method to detect changes in the soil by relating loss in contrast between successive black and white reciprocating line pairs to variations in soil transparency, induced by temperature changes in this instance.

The proposal to use pixel intensity as a measurement framework presents several challenges. Pixel intensity is sensitive to illumination levels and will vary depending on the lighting conditions provided. Moreover, individual pixels located on the camera charged couple device (CCD) sensor will be subjected to varying light intensity owing to the ability of the lens to focus light. Siemens et al. (2010) and Peters et al. (2011) encountered significant challenges when interpreting and correlating pixel intensity to saturation level as the experiment was illuminated using standard fluorescent room lighting and required the use of multiple cameras with overlapping fields of view. Hence, normalization of the pixel intensity was necessary to account for variations in illumination in the field of view due to the poor lighting conditions. In the current investigation, tests were conducted in a dark room environment under constant illumination, which significantly reduced large variations in measured pixel intensities.

Experimental Program, Apparatus and Technique

TRANSPARENT SOIL MATERIAL

The transparent soil used in this investigation consisted of 6 % fumed amorphous silica aggregate and 94 % pore fluid. The pore fluid was a blend of white oil (Baylube WOM 15) and paraffinic solvent (N-paraffin C10-13) mixed to volumetric proportions of 77:23, giving a refractive index match to the silica aggregates of 1.467 at 20°C. This ratio was previously calibrated by Stanier et al. (2012) using a visual eye chart assessment method; however, as described previously, this was superseded by a newly established quantitative framework proposed by Black and Take (2015) based on an optical calibration method known as MTF.

The particle density of the fumed silica was 2200 kg/m^3, with a surface area of 200 ± 25 m^2/g, and particle size D_{50} of 0.014 μm. The density of the fluids was measured to be 845.48 kg/m^3 for Baylube WOM 15 and 764.24 kg/m^3 for N-paraffin C10-13. The dynamic viscosity of the oils was measured using a spindle viscometer in units of centipoises (cP) and determined to be 21.2 cP and 1.2 for the Baylube and Paraffin oils, respectively, and 7.7 cP for the combined fluid mix ratio at 20°C. The volumetric coefficient of thermal expansion of paraffin oil is 7.6×10^{-4} °C^{-1}, and 4.5×10^{-4} °C^{-1} for Baylube oil.

The aggregate and pore fluid were thoroughly mixed using a hand-held food blender to produce a homogeneous slurry and then placed into the test chamber. Samples were located in a vacuum to evacuate the air to produce a two phase continuum which enabled visualization of the calibration target when placed behind the soil. The soil was consolidated to produce test beds having undrained shear strength of approximately 10 kPa for the calibration and energy pile application tests. More detailed information about the material consolidation and strength properties are described by Stanier (2011) and Kelly (2013).

TEST APPARATUS

The experimental system is portrayed in **Fig. 3** and consisted of a water bath of dimensions 600 (width) by 400 (height) by 500 mm (diameter) that provided a fluid volume capacity of approximately 100 l. A water bath was used to provide a constant temperature boundary to the submerged soil test chamber. The water bath was filled with de-aired water that was warmed using a coil heating element and water pump that circulated the water to maintain a constant temperature. Note, during calibration tests, the temperature of the water in the bath, and hence temperature of the soil, was raised at set increments ensuring thermal equilibrium was achieved at each stage. Alternatively, for the energy pile tests, the water bath was used to provide a constant boundary temperature to the submerged soil test chamber as heat was then applied directly to the energy pile.

FIG. 3 Transparent soil thermal modeling experimental setup.

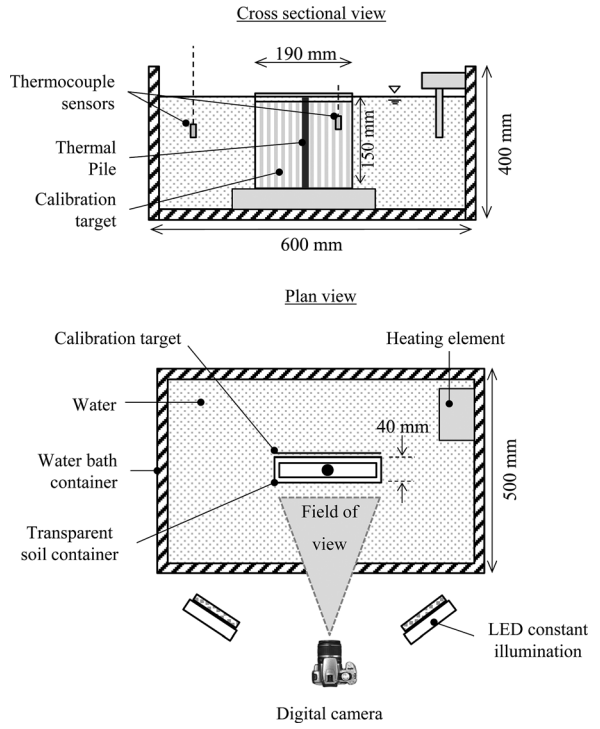

The external surfaces were covered in black card to produce a consistent background and to minimize internal light reflections. The system was instrumented with 10 LM335Z precision temperature sensors (thermocouples) that confirmed equilibrium of the water and soil temperature and to were also used to validate the image-based measurement approach.

As discussed previously, non-uniform illumination conditions are detrimental to producing consistent pixel intensity readings. For this reason, tests were conducted in a dark room environment under constant illumination provided by two LED towers. Each tower consisted of 4 individual LED panels containing 30 surface mount LEDs that were powered at 12 V dc. Light diffusers were used to disperse LED hotspots to ensure uniform illumination of the water bath and submerged soil chamber. Precursor trial tests confirmed that large variations in pixel intensity, as reported by Siemens et al. (2010) and Peters et al. (2011), did not occur and hence confirmed the suitability of the control measures implemented to minimize pixel intensity variation caused by poor illumination.

Images were captured using a Canon EOS 1100D single lens reflex (SLR) with an 18–55 mm lens. During the test, the camera was mounted on a tripod at a distance of 0.5 m from the front of the test chamber and was triggered at regular intervals using a digital signal generated from a National Instruments 6211 USB data acquisition device. This remote trigger capability ensured that it was possible to conduct long term tests without

operator intervention, which was beneficial for maintaining constant environmental conditions, and to minimize temporal movements of the camera position between successive images. In addition to illumination variation, pixel intensity can also be affected by camera parameters such as aperture, exposure time, and focus; hence, the camera properties were fixed at focal length of 55 mm, an aperture of F/16, shutter speed of 1/5th seconds, ISO of 100, auto white balance, and no flash. These parameters were optimized prior to commencing the main test schedule to yield the greatest image clarity. During testing, an image was initially captured by allowing the camera to auto focus on the target before switching to manual focus to capture the remaining test images. Images were taken at a frequency of between 1 and 10 min depending on the nature of the test, i.e., calibration or energy pile application. These rigorous precautions ensured that any changes in pixel intensity detected, subsequently interpreted as a change in soil temperature, were attributed solely to loss of transparency of the soil owing to the change in its refractive index as the soil temperature changed.

The soil test chambers used for calibration and the energy pile tests measured 190 by 150 by 40 mm and were constructed from 10-mm thick Perspex sheet. The chambers were fixed using M8 bolts and sealed using silicone sealant along the mating surfaces. During calibration, thermocouples were placed inside the chamber to provide temperature readings that were correlated with pixel intensity to verify the pixel-temperature relationship. After vacuuming, the top of the chamber was sealed using a rubber membrane held in place by a top plate. Prior to submerging in the water bath, calibration targets were prepared and waterproofed by laminating and attached to the back of the test chamber. The test chamber was located in the centre of the water bath so as to provide constant temperature boundary conditions.

The experiment was controlled and data was acquired using a National Instruments LabVIEW program that interfaced with the USB 6211 data acquisition module. The program logged thermocouple signals and triggered the camera at a user defined frequency.

CALIBRATION PROCEDURES

Calibration of pixel intensity at various soil temperatures was achieved by submerging the soil chamber in the water bath and allowing it to be heated by the re-circulating water system. Temperature stages ranged from 20 to 50°C in 5°C increments. At each stage, the temperature of the water bath was coarsely set to the desired value and the exact temperature was confirmed precisely by thermocouples submerged both in the water bath and soil. Calibration of the system confirmed the water bath was capable of heating and maintaining constant soil temperature at each incremental stage and that steady state conditions were achieved after approximately 2 h of heating exposure.

Correlation of image pixel intensity at various soil temperatures was achieved by capturing images of the calibration target placed behind the test chamber and viewed through the soil across the range of temperatures indicated. Images were captured at the end of each heating stage, ensuring that equilibrium was achieved, and also at regular intervals during the temperature ramp. Changes in soil refractive index due to temperature variations are recorded as changes in image pixel intensity. Post analysis using image processing software in Matlab enabled translation of the recorded pixel intensities to discrete temperatures using the established pixel intensity-temperature relationship described later.

ENERGY PILE APPLICATION EXAMPLE

The potential of transparent soil to visualize thermo-dynamic problems is demonstrated using an energy pile example. The pile was machined from aluminium and measured 18 mm diameter (d_0) by 150 mm long (**Fig. 4**). A cartridge heating element, 6.5 mm in diameter by 70 mm long, was inserted in a bored recess in the centre of the pile and fixed in place using thermal epoxy. The heating element had a power rating of 100 W and was interfaced with a CAL 3300 proportional-integral-derivative (PID) relay temperature controller that used feedback from a thermocouple embedded on the surface of the pile to regulate temperature to within ±0.5°C. The pile was sprayed matte black to minimize reflections into the soil and also ensure that changes in pixel intensity at the pile–soil interface would be clearly identifiable.

Energy pile tests were conducted by increasing the temperature of the pile to 50°C, while maintaining the temperature of the water bath at 20°C. Typical in situ ground temperatures are in the range of 10°C–15°C, thus the selected valued of 20°C is

FIG. 4 Energy pile application (*a*) energy pile, (*b*) test chamber with vertical stripe and uniform black calibration target regions, and (*c*) concentric circles and uniform black calibration target.

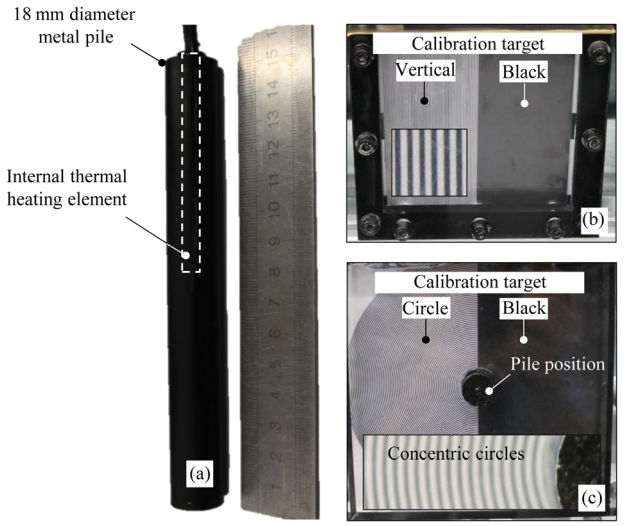

FIG. 5

Calibration of experimental system (*a*) temperature response over the entire temperature range from 20 to 50°C and (*b*) water bath and soil temperature response for 20°C to 25°C temperature increment.

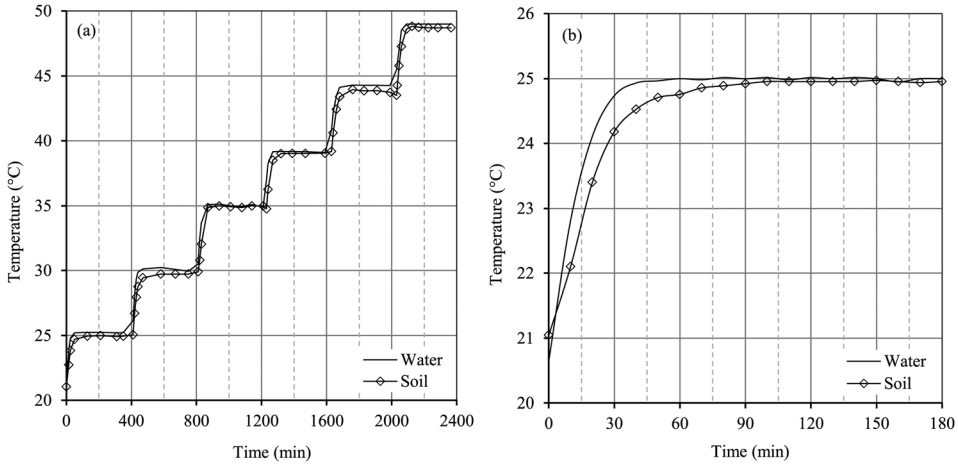

slightly higher than what may normally be expected. However, higher temperatures in the region of 18°C–20°C were reported by Bourne-Webb et al. (2009), believed to be due to heat radiating from other underground infrastructure; hence, 20°C for the ambient soil temperature was considered viable for the preliminary experimental test. This was also advantageous as the laboratory environment was maintained at a temperature of 20°C.

Two pile orientations were considered to show the impact of temperature change and heat flow (i) vertically in the middle of the test chamber to examine the temperature along its length and (ii) horizontally (i.e., end on to the camera principle axis) to evaluate the radial zone of influence. In the case of the vertical pile, the black and vertical stripe calibration target was used; however, for the horizontally placed pile, a specially adapted target was created whereby the vertical lines were changed to concentric circles radiating from the pile centre at the line spacing of 1 lp/mm (**Fig. 4(c)**).

Results and Discussion

A number of tests were conducted to verify the experimental methodology, calibration of pixel intensity with temperature, and to demonstrate the potential of this new approach. The main purpose of this paper is to confirm the hypothesis that transparent soil can be used for thermo-dynamic modeling using image-based measurement based on pixel intensity. Note, the energy pile example is provided to demonstrate the potential of this technique to visualize heat flow in and thermal flow processes and not to provide definitive insight of energy pile behavior at this stage. This would require additional testing and verification, which is beyond the scope of this paper.

CALIBRATION OF THE TEST ENVIRONMENT

The test environment was calibrated by increasing the temperature of the water in the bath and logging the temperature response of the thermocouples. This process was conducted several times, placing the sensors in different locations, to verify the time required to regulate the temperature and confirm that uniform temperature conditions were maintained. The water bath reached a steady temperature after approximately 200 min (**Fig. 5(*a*)**) that was also verified independently using a thermometer. In some stages, the final temperature of the water did not precisely reach the desired global value owing to thermal losses from the sides and top of the water bath and the accuracy of the heating coil thermostat. This problem was more pronounced at elevated temperatures above 35°C due to the higher temperature differential of the water relative to the laboratory environment that was controlled at 20°C. This was not considered detrimental to the establishment of a pixel–temperature relationship, as the temperature did reach a point of equilibrium, albeit not precisely the desired value. Moreover, the temperature–pixel relationship was derived using the more accurate thermocouple measurement captured within the soil.

Some lag was observed in the rate at which the water and soil heated owing to the difference in the thermal conductivity of the water, soil test chamber and soil (**Fig. 5(*b*)**). The thermal conductivity (k) of water and Perspex are approximately $0.56\,W \cdot m^{-1} \cdot k^{-1}$ and $0.17\,W \cdot m^{-1} \cdot k^{-1}$, respectively. A series of tests on the transparent soil using a KD2Pro thermal needle probe indicated it had a thermal conductivity of $0.33\,W \cdot m^{-1} \cdot k^{-1}$ for the density and saturation conditions tested. This is lower than typical values reported for soils in literature, in the region of $0.7–1.5\,W \cdot m^{-1} \cdot k^{-1}$ for sand and clay, respectively (Busby et al. 2009); nevertheless, it was still suitable to model thermo-dynamic problems.

PIXEL INTENSITY AND TEMPERATURE RELATIONSHIP

Captured images were processed using Matlab as this program allowed interrogation of pixel intensities. Despite the improved illumination conditions in the current tests, small variations of

up to 10 pixels were observed in pixel intensity measurements across the calibration target in images captured at the extreme 20 and 50°C temperatures. This is significantly lower than the maximum deviation of approximately 50 pixels reported by Peters et al. (2010); however, it still represents a potential error over the pixel range. Any variation in pixel intensity will have a detrimental effect on the interpretation of temperatures using an image-based measure detection system. Hence, pixel intensity normalization was conducted to account for the small anomalies observed at each pixel location using the minimum and maximum intensities determined for images at the extreme temperatures of 20 and 50°C according to Eq 1:

$$PI_N = \frac{PI - PI_{\min}}{PI_{\max} - PI_{\min}} \quad (1)$$

where:

PI_N = the normalised pixel intensity,

PI = the captured intensity at a given temperature, and

PI_{min} and PI_{max} = the minimum and maximum pixel intensity recorded at 20 and 50°C, respectively.

This normalization was implemented for each temperature increment such that the normalized pixel intensity of the soil varied from 0 to 1 for temperatures of 20 and 50°C, respectively.

The resulting normalized pixel intensity of the uniform black region of the calibration target was correlated with the thermocouple temperature measurements and is displayed in **Fig. 6**. A strong correlation relating normalized pixel intensity with temperature is evident, with low levels of data scatter present. Between 20 and 30°C, the normalized relationship is non-linear beyond which a linear relation is apparent; although it is not established whether a linear trend will continue over a greater range of temperatures. It is also interesting to note that the trend line turning point corresponds to the temperature at which the material was calibrated to yield optimum transparency (i.e., 20°C). This is in good agreement with previous research reported by Stanier (2011) and Black and Take (2015), and provides further confidence in the pixel intensity–temperature relationship established and presented in **Fig. 6**. This relationship confirms the hypothesis for an image-based measurement approach to observe temperature changes in transparent soil. This discovery presents an exciting new opportunity for transparent soil to contribute to modeling thermo-dynamic processes in soils.

FIG. 6 Normalized pixel intensity with increasing soil temperature.

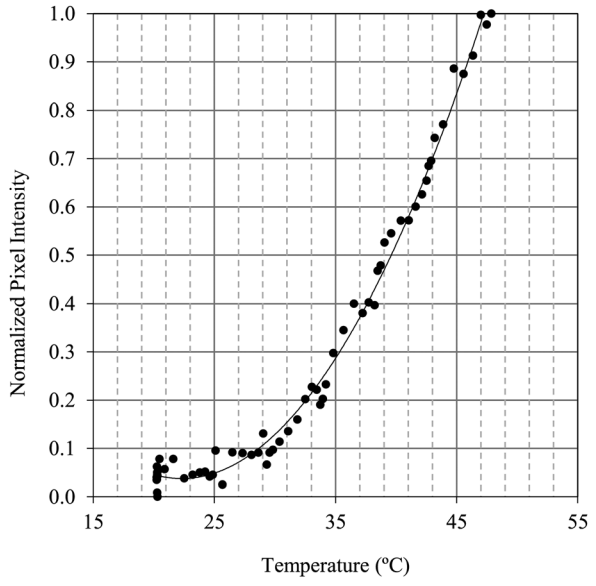

ENERGY PILE APPLICATION

The emerging application of an energy pile has been selected to demonstrate the potential of transparent soil and this newly established relationship to model thermo-dynamic processes. Tests were conducted in accordance with the procedure outlined in the section "Energy Pile Application Example." **Figure 7** presents analysis of the soil temperature response for an energy pile vertically embedded in the soil during which the temperature of the pile was activated and increased to a constant temperature of 50°C. Data is presented at time intervals of 10, 30, 60, and 120 min, beyond which no further changes were detected; radial distance away from the pile centreline and depth are normalized by the pile diameter. The heat map shows regions of varying soil temperature and is presented in °C by converting the recorded image pixel intensities using the previously established relationship for normalized pixel intensity and temperature.

Horizontal heat flow propagating radially from the pile is clearly evident. At $t = 10$ min, only a small region of soil to a depth $z/d_0 = 3$ exhibits an increase in temperature of approximately 35°C. This corresponds with the location of the internal heating element embedded in the pile that extended to a depth corresponding to $z/d_0 = 4$. Significant changes are observed with longer heating exposure time, whereby increased soil temperature is clearly evident along the entire length of the pile. Some small temperature rise is also registered at the pile base. It is also interesting to note that greater thermal heating continues to occur in the upper region of the pile near the heat source. A clear thermal gradient is establish at $t = 30$ min, whereby the temperature at the pile–soil interface is the same as the pile at 50°C, and decreases with distance from the pile centreline to the ambient soil background temperature of 20°C that is maintained by the water bath boundary condition. The extent to which this heating zone extends continues to grow up to $t = 120$ min, at which point no further changes were detected. The zone of heating in the soil at the steady state conditions varies slightly along the pile depth from approximately $r/d_0 = 1.5$ up to a depth of $z/d_0 < 3$, to $r/d_0 = 1.0$ at $z/d_0 > 7$. It is

FIG. 7 Horizontal heat flow visualized in transparent soil along the pile length for a 20°C–50°C heating cycle at time intervals t = 10, 30, 60, and 120 min depicted as a thermal heat map.

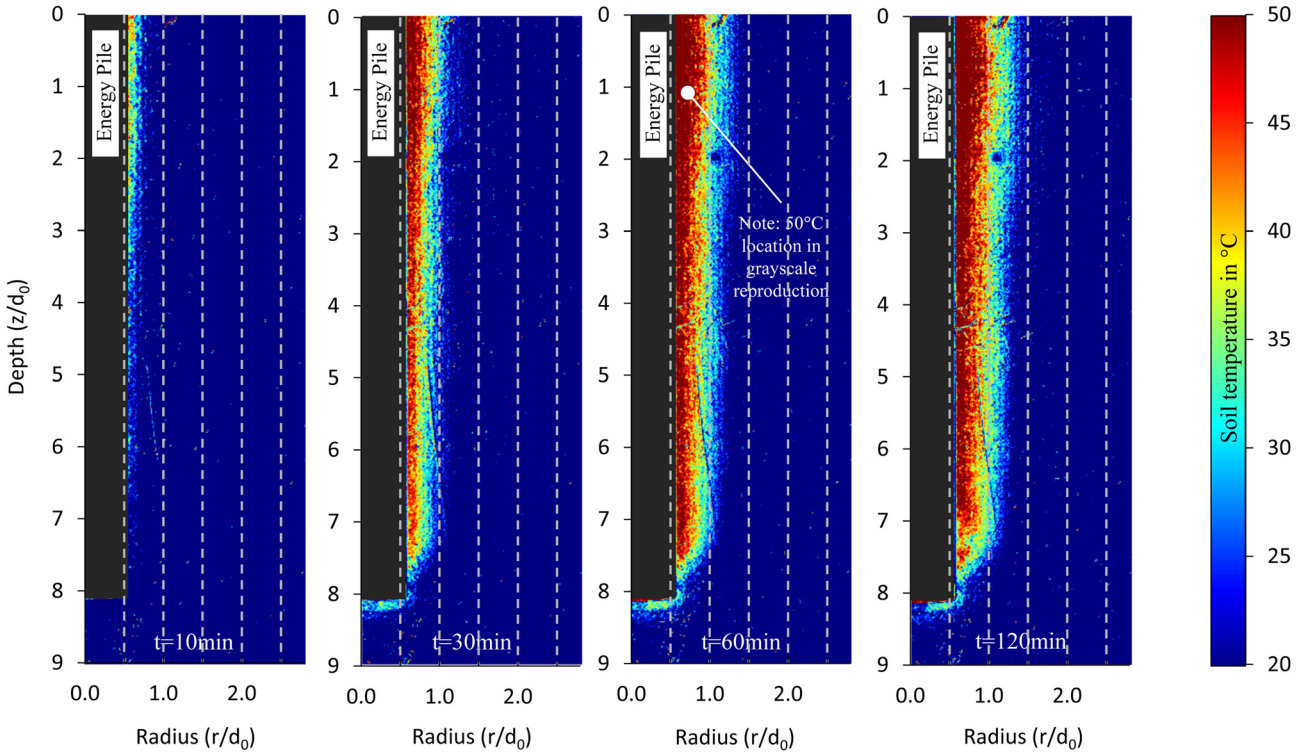

these observed changes in soil temperature along the length of an energy pile that have been postulated by Laloui et al. (2006), Bourne-Webb et al. (2009), and Brandl (2006) as the likely contributing factor for increased foundation movements in geothermal structures due to changes in side friction characteristics arising from thermal expansion and contraction of the soil. Note, the load–displacement performance of the pile or the volumetric response of the soil was not considered in this study; thus, the latter postulation remains an area for further investigation.

The zone of heating influence is more readily portrayed when the pile is viewed end on, as shown in **Fig. 8**. A second

FIG. 8 Radial heat flow visualized in transparent soil at a pile cross section depth $z/d_0 = 7$, for a 20°C–50°C heating cycle at time intervals t = 10, 30, 60, and 120 min, depicted as a thermal heat map.

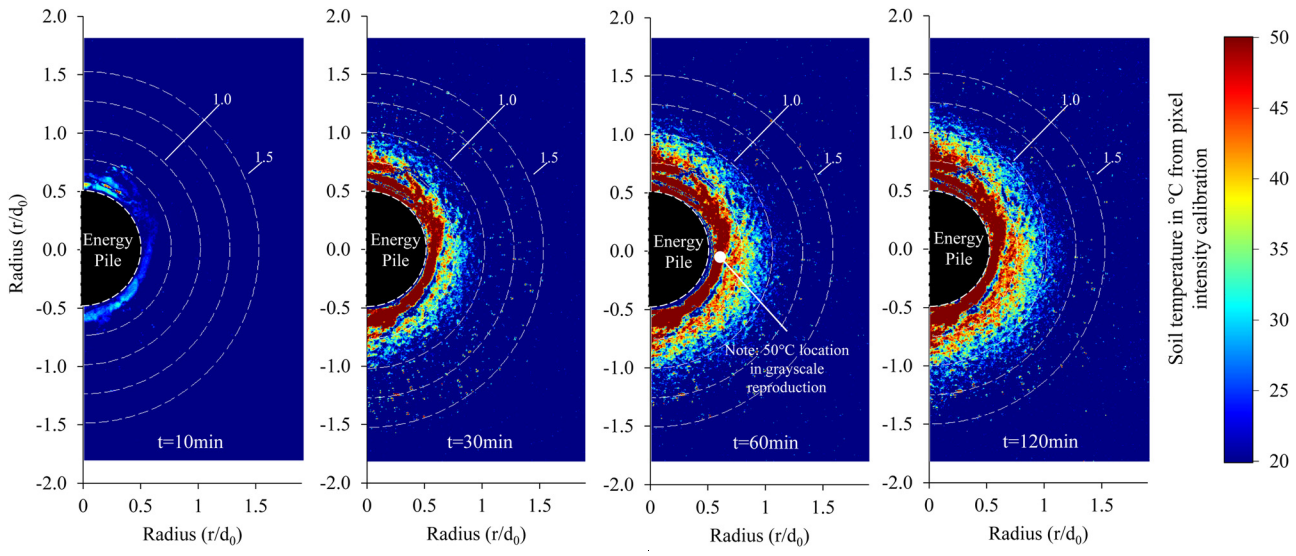

FIG. 9

Zone of influence of heating for a single energy pile determined by signal modulation for a 20°C–50°C heating cycle at $t = 0$ and 120 min; (*a*) image showing loss of optical transmission of the concentric black/white reference lines, (*b*) signal modulation and (*c*) normalized zone of heating influence.

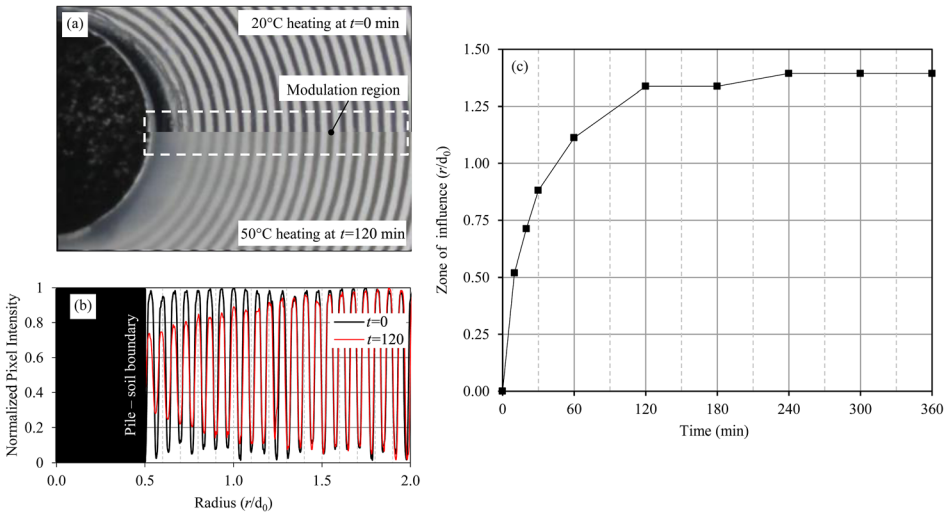

pile test was conducted to examine a cross section of the pile at a pile depth of $z/d_0 = 7$, for the same time increments of $t = 10$ to 120 min. The horizontal and vertical axis are normalized by the pile diameter. During heating, a clear zone of soil up to $r/d_0 = 0.75$ can be seen to be heated to 50°C, which reduces steadily in temperature up to $r/d_0 = 1.25$. Beyond this radial distance, the soil temperature is relatively unaffected.

While **Fig. 7** and **Fig. 8** offers a striking visual portrayal of the soil temperature and thermal gradient, it is difficult to assess the exact zone of heating influence owing to the gradual transition in temperature that occurs. For this purpose, the black and white striped target was used to examine the signal modulation of low and high contrast to ascertain the extent of heating. **Figure 9** presents images of the concentric black and white circular target at 20 and 50°C, where it is evident that the lines are less distinct at 50°C when the refractive index changed from the calibrated value. This loss in optical transmission is confirmed by the signal modulation spectrum, which appears smaller at the pile interface. As the radial distance increases, the modulation of the normalized pixel intensity amplifies, indicating that the soil refractive index has been less affected by a change in temperature. The signal modulation recovers at approximately $r/d_0 = 1.3$ to match the signature obtained at 20°C, which indicates the heating zone of influence for the energy pile. This method was implemented to determine the increase in the zone of influence with increased time.

Bourne-Webb et al. (2009) reported that the temperature recorded in a borehole positioned 0.5 m from the energy pile halved at a radial distance equivalent to $r/d_0 = 1$ and at $r/d_0 = 1.5$ changes where negligible. Cui et al. (2011) reported $r/d_0 = 1.2$ for the zone of influence from a numerical analysis of a pile geothermal heat exchanger. Although similar zones of influence are observed in the present work, scaling of heat flow from small scale models to prototype field conditions is highly complex. For example, Savvidou (1988) presents a comprehensive investigation pertaining to the modelling of heat flow in soils. Derivation of scaling laws for conduction and convection are presented and verified by results from model experiments conducted on saturated Leighton Buzzard sand at 1 and 100 g in a centrifuge. Comparison of models at 1g and Ng demonstrated that distinct differences in the heat transfer mechanism occurred; convection was dominant in centrifuge tests, whereas conduction is more significant at 1 g. Hence, based on the complexity associated with modelling heat transfer, it would be inappropriate at this stage to make direct comparisons and draw conclusions with field-based data arising from the embryonic methodology presented in this paper. The authors advocate that considerably more knowledge about the heat transfer mechanisms and associated scaling laws of transparent soil are required before such comparisons could be made. Nevertheless, despite some uncertainties in the correlation with full-scale field behavior, the work has successfully introduced a new modelling paradigm for transparent soil, and with further research, the investigative method could enable new insight and make a positive contribution in modelling thermo-dynamic problems in soil.

Conclusions

Managing energy resources is fast becoming a crucial issue of the 21st century, with geothermal heat exchange energy structures targeted as a viable means of reducing carbon emissions associated with regulating building temperatures. An alternative experimental method using transparent soil and digital image analysis is presented for the purpose of visualizing heat flow in soil. The research shows that the loss of optical clarity can be used as a beneficial attribute of transparent soil. The work explored and verified the hypothesis that temperature changes of the soil alter its refractive index and therefore progressively reduce its

transparency, becoming more opaque. The development of the experimental methodology was discussed and a relationship between pixel intensity and soil temperature is defined and verified. Normalization of pixel intensities was conducted to mitigate changes in illumination observed in the calibration target. This relationship is applied to an energy pile example in heating mode to demonstrate and visualize heat flow in soil. The heating zone of influence is observed to extend to a radial distance of 1.5 pile diameters, which reflects similar values reported in literature from field and numerical investigations. The paper reported on the successful implementation of this technique, which provides a new paradigm for transparent soil to potentially contribute to greater understanding of thermo-dynamic processes in soil. Although focused on thermal heating, additional works by the authors into cooling effects on transparent soil show early promise that the same experimental framework can be used to investigate cooling problems below ambient temperatures, which may enable both heating and cooling problems to be simulated.

References

Ahmed, M. and Iskander, M., 2010, "Analysis of Tunnelling Induced Ground Movements Using Transparent Soil Models," *J. Geotech. Geoenviron. Eng.*, Vol. 137, No. 5, pp. 525–535.

Black, J. A., 2012, "Ground displacement during press-in piling using transparent soil and PIV," presented at the *International Press-In Association, 4th IPA Workshop*, Singapore, Dec 6–7, International Press-In Association, Tokyo, Japan, pp. 1–8.

Black, J. A. and Take, W., 2015, "Quantification of Optical Clarity of Transparent Soil Using the Modulation Transfer Function," *ASTM Geotech. Test. J.* (accepted).

Boudali, M., Leroueil, S., and Srinivasa Murthy, B. R., 1994, "Viscous Behaviour of Natural Clays," *Proceedings of the 13th International Conference on Soil Mechanics and Foundation Engineering*, Vol. 1, New Delhi, India, Jan 5–10, CRC Press, Boca Raton, FL, pp. 411–416.

Bourne-Webb, P. J., Amatya, B., Soga, K., Amis, T., Davidson, C., and Payne, P., 2009, "Energy Pile Test at Lambeth College, London: Geotechnical and Thermodynamic Aspects of Pile Response to Heat Cycles," *Geotechnique*, Vol. 59, No. 3, pp. 237–248.

Brandl, H., 2006, "Energy Foundations and Other Thermo-Active Ground Structures," *Geotechnique*, Vol. 56, No. 2, pp. 81–122.

Britto, A., Savvidou, C., Maddocks, D., Gunn, M., and Booker, J., 1989, "Numerical and Centrifuge Modelling of Coupled Heat Flow and Consolidation Around Hot Cylinders Buried in Clay," *Geotechnique*, Vol. 39, No. 1, pp. 13–25.

Busby, J., Lewis, M., Reeves, H., and Lawley, R., 2009, "Initial Geological Considerations Before Installing Found Source Heat Pump Systems," *Q. J. Eng. Geol. Hydrogeol.*, Vol. 46, No. 2, pp. 295–306.

Campanella, R. G. and Mitchell, J. R., 1968, "Influence of Temperature Variations on Soil Behaviour," *ASCE J. Soil Mech. Found. Div.*, Vol. 94, No. 3, pp. 709–734.

Cekerevac, C. and Laloui, L., 2004, "Experimental Study of Thermal Effects on the Mechanical Behaviour of a Clay," *Int. J. Numer. Anal. Methods Geomech.*, Vol. 28, No. 11, pp. 209–288.

Cui, P., Li, X., Man, Y., and Fang, Z., 2011, "Heat Transfer Analysis of Pile Geothermal Heat Exchanges With Spiral Coils," *Appl. Energy*, Vol., 88, No. 11, pp. 4113–4119.

Demars, K. R. and Charles, R. D., 1982, "Soil Volume Changes Induced by Temperature Cycling," *Can. Geotech. J.*, Vol. 19, No. 2, pp. 188–194.

Ezzein, F. and Bathurst, R. J., 2014, "A New Approach to Evaluate Soil–Geosynthetic Interaction Using a Novel Pullout Test Apparatus and Transparent Granular Soil," *Geotext. Geomembr.*, Vol. 42, No. 3, pp. 246–255.

Forlati, G. and Black, J. A., 2014, "Impact of Pile Geometry on the Installation of Open Ended Press-In Piles," *Proceedings of the 8th International Conference on Physical Modeling in Geotechnics*, Perth, Australia, Jan 14–17, CRC Press, Boca Raton, FL, pp. 763–769.

Gao, J., Zhang, X., Liu, J., Li, K., and Yang, J., 2008, "Thermal Performance and Ground Temperature of Vertical Pile-Foundation Heat Exchangers: A Case Study," *Appl. Energy*, Vol. 86, Nos. 17–18, pp. 2295–2304.

Gill, D., 1999, "Experimental and Theoretical Investigations of Pile and Penetrometer Installation in Clay," Ph.D. thesis, Trinity College, Dublin, Ireland.

Goode, J., III, Zhang, M., and McCartney, J. S., 2014, "Centrifuge Modeling of Energy Foundations in Sand and Clay," *Proceedings of the 8th International Conference on Physical Modelling in Geotechnics*, Perth, Australia, Jan 14–17, CRC Press, Boca Raton, FL, pp. 729–735.

Habibagahi, K., 1977, "Temperature Effects and the Concept of Effective Void Ratio," *Ind. Geotech. J.*, Vol. 7, No. 1, pp. 14–34.

Hepbasli, A., Akdemir, O., and Hancioglu, E., 2003, "Experimental Study of a Closed Loop Vertical Ground Source Heat Pump System," *Energy Conserv. Manage.*, Vol. 44, No. 4, pp. 527–548.

Hird, C., Ni, Q., and Guymer, I., 2008, "Physical Modeling of Displacements Around Continuous Augers in Clay," *Proceedings of the 2nd British Geotechnical Association International Conference on Foundations*, Vol. 1, Dundee, UK, June 24–27, IHS Bre Press, Berkshire, UK, pp. 565–574.

Houston, S. L., Houston, W. N., and Williams, N. D., 1985, "Thermo-Mechanical Behaviour of Seafloor Sediments," *J. Geotech. Eng.*, Vol. 111, No. 11, pp. 1249–1263.

Hueckel, T. and Baldi, G., 1990, "Thermoplasticity of Saturated Clays: Experimental Constitutive Study," *J. Geotech. Eng.*, Vol. 116, No. 2, pp. 1778–1796.

Hueckel, T., Francois, B., and Laloui, L., 2011, "Temperature-Dependent Internal Friction of Clay in a Cylindrical Heat Source Problem," *Geotechnique*, Vol. 61, No. 10, pp. 831–844.

Hueckel, T. and Pellegrini, R., 1992, "Effective Stress and Water Pressure in Saturated Clays During Heating–Cooling Cycles," *Can. Geotech. J.*, Vol. 29, No. 6, pp. 1095–1102.

Hueckel, T., Laloui, L., and Francois, B., 2009, "Implications of Thermal Sensitivity of the Static Internal Friction Angle," *Proceedings of the 1st International Symposium on Computational Geomechanics*, Juan les Pins, France, April 29–May 1, International Center of Computational Engineering, Rhodes, Greece, pp. 104–115.

Iskander, M., 2010, *Modeling With Transparent Soils: Visualizing Soil Structure Interaction and Multi Phase Flow, Non-Intrusively*, Springer, New York.

Iskander, M., Lai, J., Oswald, C., and Mannheimer, R., 1994, "Development of a Transparent Material to Model the Geotechnical Properties of Soils," *ASCE Geotech. Test. J.*, Vol. 17, No. 4, pp. 425–433.

Iskander, M., Liu, J., and Sadek, S., 2002, "Transparent Amorphous Silica to Model Clay," *J. Geotech. Geoenviron. Eng.*, Vol. 128, No. 3, pp. 262–273.

Kelly, P., 2013, "Soil Structure Interaction and Group Mechanics of Vibrated Stone Column Foundations," Ph.D. thesis, University of Sheffield, Sheffield, UK.

Laloui, L., Moreni, M., and Vulliet, L., 2003, "Behavior of a bifunctional pile, foundation and heat exchanger," *Can. Geotech. J.*, Vol. 40, No. 2, pp. 388–402 (in French).

Laloui, L., Nuth, M., and Vulliet, L., 2006, "Experimental and Numerical Investigations of the Behaviour of a Heat Exchanger Pile," *IJNAMG*, Vol. 30, No. 8, pp. 763–781.

Liu, J., Iskander, M., and Sadek, S., 2002, "Optical Measurement of Deformation Under Foundations Using a Transparent Soil Model," *International Conference on Physical Modeling in Geotechnics: ICPMG*, St. Johns, Newfoundland, Canada, July 10–12, CRC Press, Boca Raton, FL, pp. 155–159.

Liu, J., Iskander, M., and Sadek, S., 2003, "Consolidation and Permeability of Transparent Amorphous Silica," *ASCE Geotech. Test. J.*, Vol. 26, No. 4, pp. 1–12.

Loveridge, F. and Powrie, W., 2012, "Pile Heat Exchangers: Thermal Behavior and Interactions," *Proc. Inst. Ci.v Eng., Ground Eng.*, Vol. 166, No. 2, pp. 178–196.

Mitchell, J. K., 1964, "Shearing Resistance of Clay as a Rate Process," *ASCE J. Soil Mech. Found. Div.*, Vol. 90, No. 1, pp. 29–61.

Ng, C. W. W., Shi, C., Gunawan, A., and Laloui, L., 2014, "Centrifuge Modelling of Energy Piles Subjected to Heating and Cooling Cycles in Clay," *Geotech. Lett.*, Vol. 4, No. 4, pp. 310–316.

Pahud, D., and Hubbuch, M., 2007, "Measured Thermal Performances of the Energy Pile System of Dock of the Midfield at Zurich Airport," presented at the *Proceedings of the European Geothermal Congress*, Unterhaching, Germany, 30th May–1st June, Unterhaching, Germany, -unpublished.

Peters, S. B., Siemens, G., and Take, W. A., 2011, "Characterization of Transparent Soil for Unsaturated Applications," *ASTM Geotech. Test. J.*, Vol. 34, No. 5, pp. 445–456.

Plum, R. L. and Esrig, M. I., 1969, "Some Temperature Effects on Soil Compressibility and Pore Water Pressure, Effects of Temperature and Heat on Engineering Behaviour of Soils," *Highw. Res. Board*, Vol. 103, pp. 231–242.

Sadek, S., Iskander, M., and Liu, J., 2002, "Geotechnical Properties of Transparent Silica," *Can. Geotech. J.*, Vol. 39, No. 1, pp. 111–124.

Sadek, S., Iskander, M., and Liu, J., 2003, "Accuracy of Digital Image Correlation for Measuring Deformations in Transparent Media," *ASCE J. Comput. Civ. Eng.*, Vol. 17, No. 2, pp. 88–96.

Savvidou, C., 1988, "Centrifuge Modelling of Heat Transfer in Soil," *Proceedings International Conference Centrifuge* 88, Paris, France, April 25–27, J. F. Corté, Ed., Balkema, Rotterdam, the Netherlands, pp. 583–591.

Siemens, G., Peters, S., and Take, W. A., 2010, "Analysis of a Drawdown Test Displaying the Use of Transparent Soil in Unsaturated Flow Applications," *Proceedings of the 5th International Conference on Unsaturated Soils*, Barcelona, Spain, Sept 6–8, Taylor & Francis, London, pp. 733–738.

Stanier, S. A., 2011, "Modeling the Behaviour of Helical Screw Piles," *Ph.D. thesis*, University of Sheffield, Sheffield, UK.

Stanier, S. A., Black, J. A., and Hird, C. C., 2012, "Enhancing Accuracy and Precision of Transparent Synthetic Soil Modeling," *Int. J. Phys. Model. Geotech.*, Vol. 12, No. 4, pp. 162–175.

Stanier, S. A., Black, J. A., and Hird, C. C., 2013, "Modeling Helical Screw Piles in Clay and Design Implications," *Proc. Inst. Civ. Eng.: Geotech. Eng.* (available online).

Stewart, M. A. and McCartney, J. S., 2012, "Strain Distributions in Centrifuge Model Energy Foundations," presented at the *ASCE GeoCongress 2012*, Oakland, CA, March 25–29, ASCE, Reston, VA, -unpublished.

Stewart, M. A. and McCartney, J. S., 2014, "Centrifuge Modelling of Soil–Structure Interaction in Energy Foundations," *J. Geotech. Geoenviron. Eng.*, Vol. 140, No. 4, 04013044.

Towhata, I., Kuntiwattanaul, P., Seko, I., and Ohishi, K., 1993, "Volume Change of Clays Induced by Heating as Observed in Consolidation Tests," *Soils Found.*, Vol. 33, No. 4, pp. 170–183.

Wood, C. J., Liu, H., and Riffat, S. B., 2010, "An Investigation of the Heat Pump Performance and Ground Temperature of a Pile Foundation Heat Exchanger System for a Residential Building," *Energy*, Vol. 35, No. 12, pp. 3932–3940.